Galactic Correlates of SMBH Growth from 25 Years of Chandra and XMM-Newton

W.N. Brandt (Penn State)

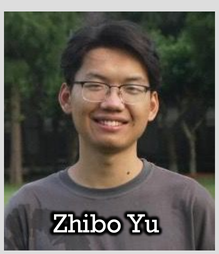

- Galaxy stellar mass (M_*)
- Star-formation rate (SFR)
- Compactness (e.g., Σ_1)
- Local (sub-Mpc) environment
- Global (1-10 Mpc) environment
- Stellar-population age

Surveys Used and Techniques

Table 1. Basic Information for the Fields Used in This Work

Field	Area (deg^2)	m_{lim} (AB mag)	X-ray Depth (ks)	X-ray ref.	Galaxy ref.	Photo-z ref.	AGN	Galaxies	(a, b)
(1)	(2)	(3)	(4)	(5)	(6)	(7)	(8)	(9)	(10)
GOODS-S	0.05	26.5 (H)	7000 (Chandra)	5	1	4,8	224 (111)	4144	(−15.87, 2.63)
GOODS-N	0.05	26.5 (H)	2000 (Chandra)	8	1	1,11	174 (167)	4603	(−15.49, 2.58)
EGS	0.06	26.5 (H)	800 (Chandra)	6	1	9	112 (10)	5889	(−15.13, 3.08)
UDS	0.06	26.5 (H)	600 (Chandra)	4	1	8	117 (25)	5010	(−15.05, 4.90)
COSMOS	1.27	24 (K_s)	160 (Chandra)	3	2	5,10	1459 (880)	86765	(−14.68, 5.19)
ELAIS-S1	2.93	23.5 (K_s)	30 (XMM-Newton)	7	3	6,12	676 (261)	157791	(−13.90, 4.57)
W-CDF-S	4.23	23.5 (K_s)	30 (XMM-Newton)	7	3	6,12	872 (311)	210727	(−13.86, 4.97)
XMM-LSS	4.20	23.5 (K_s)	40 (XMM-Newton)	2	3	2	1765 (898)	254687	(−14.09, 5.36)
eFEDS	59.75	22 (Z)	2 (eROSITA)	1	2	3,7	2667 (1156)	615068	(−13.51, 2.59)

Wedding-cake surveys design

Up to 8000 AGNs in 1.3 million galaxies

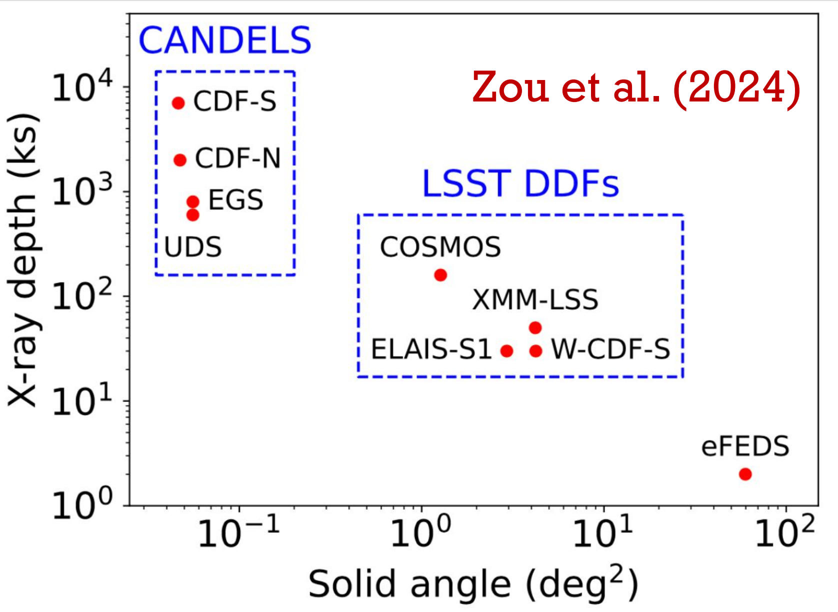

Long-term SMBH growth traced with the X-ray data, by averaging over samples.

Galaxy properties measured from the extensive multiwavelength data via, e.g., FIR-to-X-ray SED fitting.

Non-parametric partial-correlation analyses used to determine what correlations are fundamental.

The Chandra Deep Fields

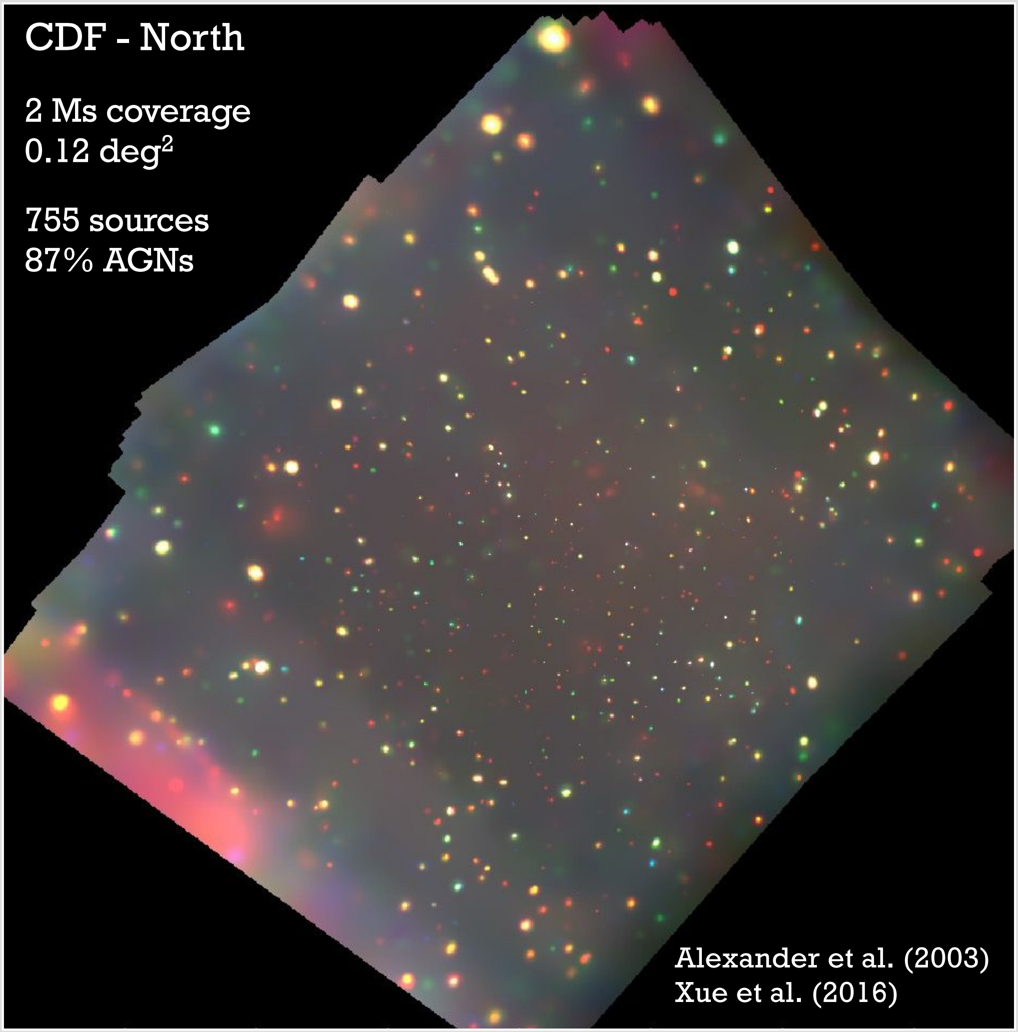

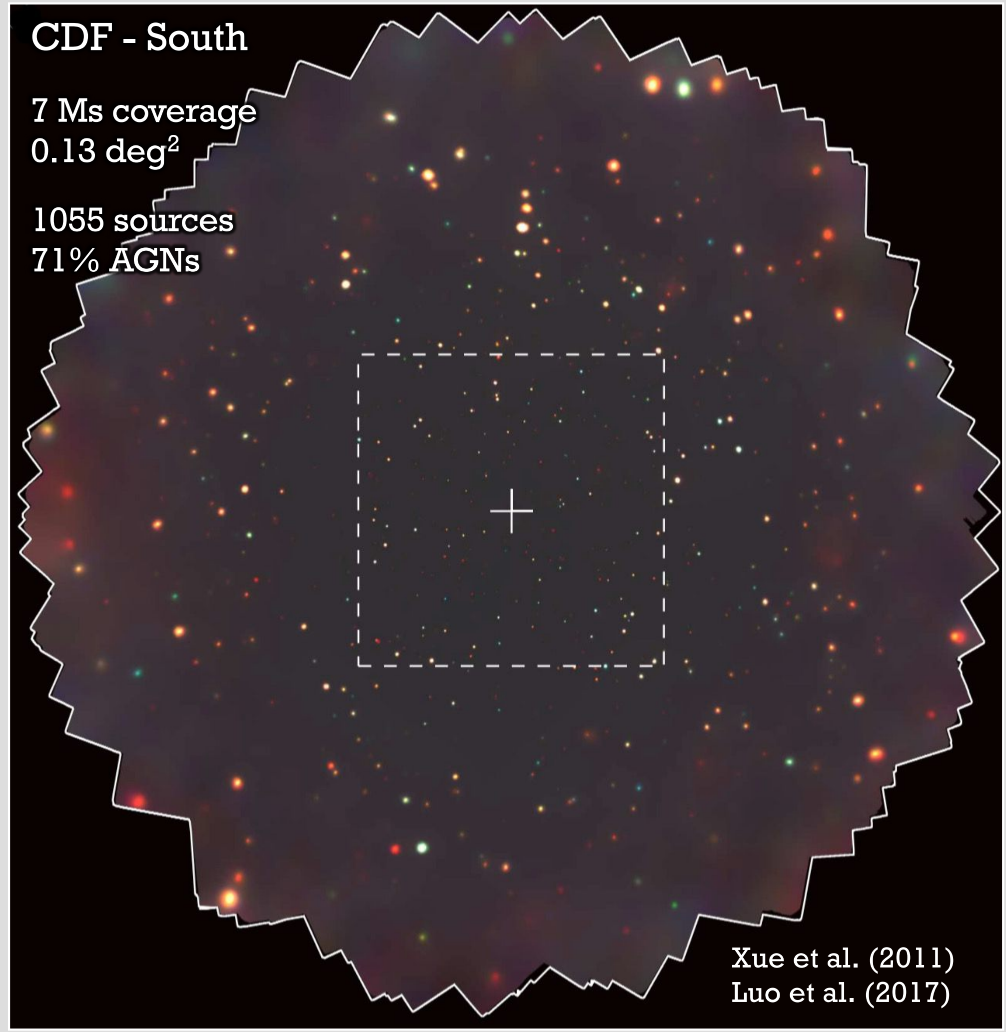

XMM-SERVS Heritage Program

Chen et al. (2018); Ni et al. (2021)

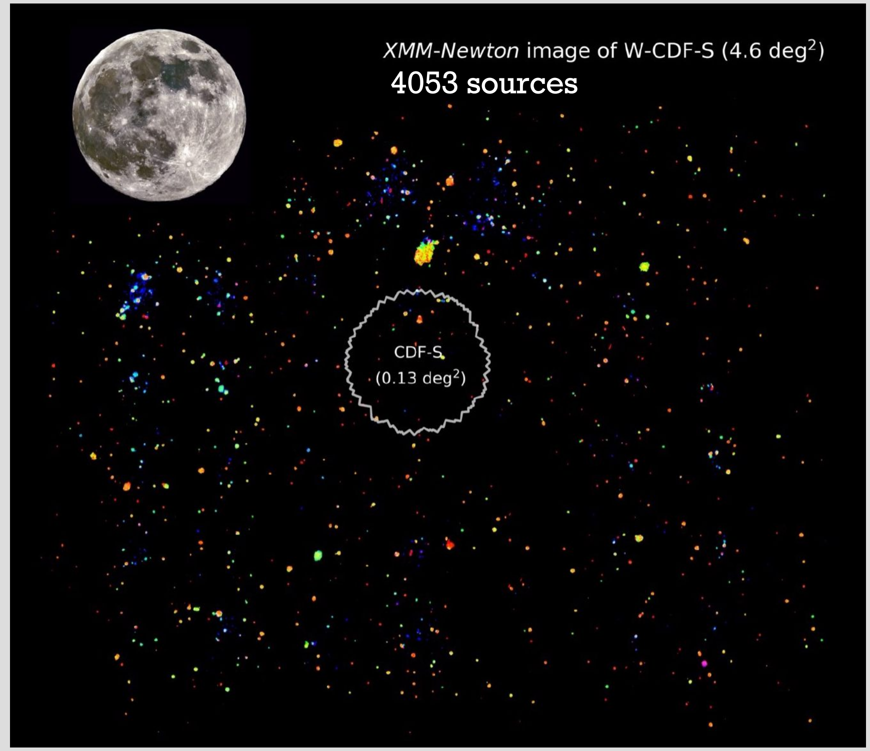

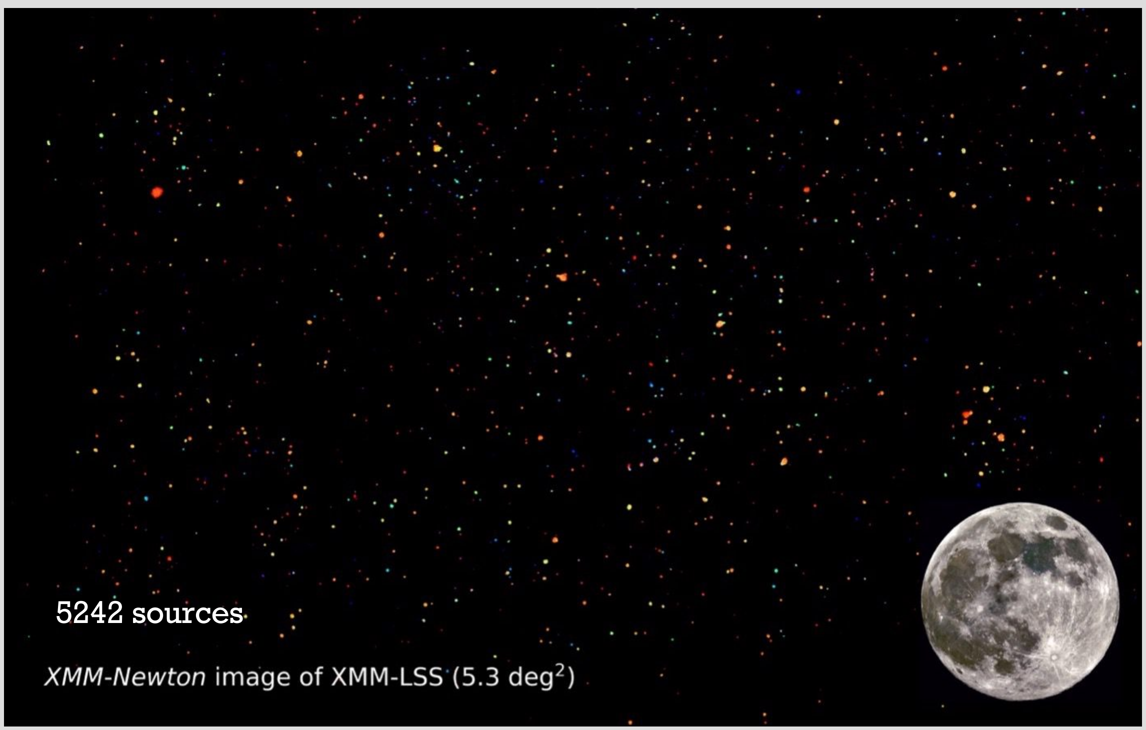

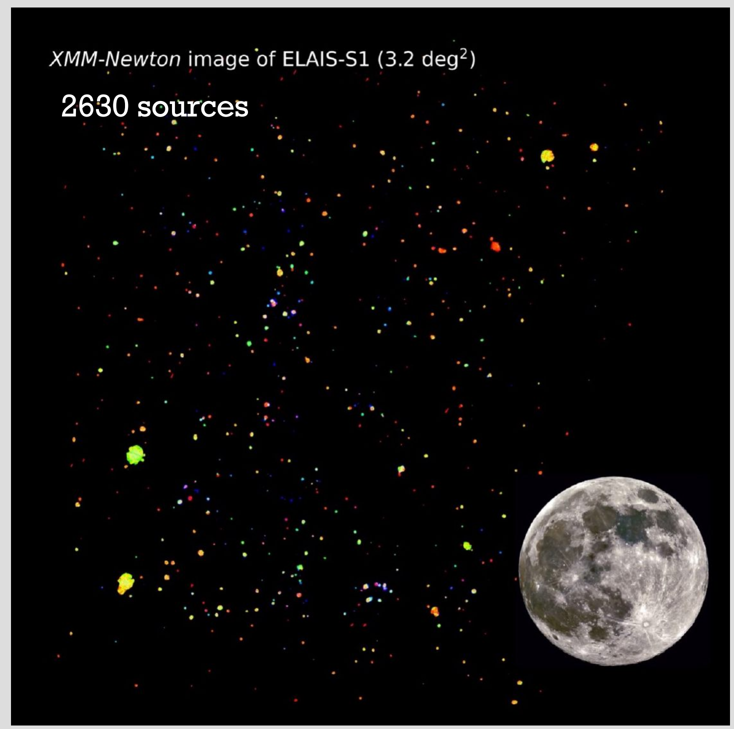

eROSITA eFEDS Field

140 deg^2 – we use the best 60 deg^2 e.g., Brunner et al. (2023)

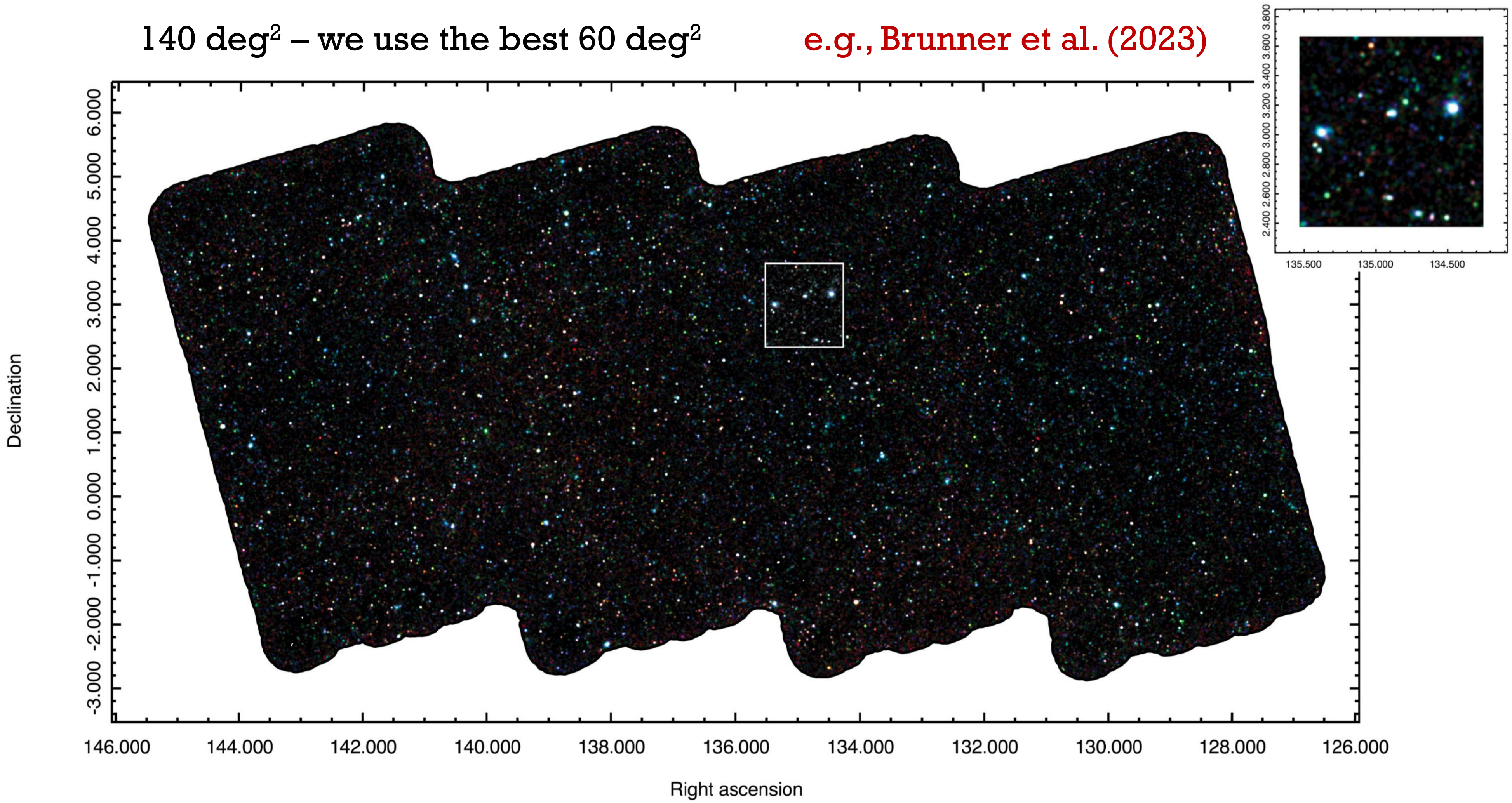

Fig. 2. RGB image of the eFEDS field in X-rays, created using 0.2–0.5 (R), 0.5–1 (G), and 1–2 (B) keV bands. Each count rate image has been smoothed with a Gaussian with $\sigma = 10$ pixels (40″). The inset in the upper right corner shows a zoom-in around a newly discovered supercluster (Liu et al. 2022a).

Surveys Used and Techniques

Table 1. Basic Information for the Fields Used in This Work

Field	Area (deg^2)	m_{lim} (AB mag)	X-ray Depth (ks)	X-ray ref.	Galaxy ref.	Photo-z ref.	AGN	Galaxies	(a, b)
(1)	(2)	(3)	(4)	(5)	(6)	(7)	(8)	(9)	(10)
GOODS-S	0.05	26.5 (H)	7000 (Chandra)	5	1	4,8	224 (111)	4144	(−15.87, 2.63)
GOODS-N	0.05	26.5 (H)	2000 (Chandra)	8	1	1,11	174 (167)	4603	(−15.49, 2.58)
EGS	0.06	26.5 (H)	800 (Chandra)	6	1	9	112 (10)	5889	(−15.13, 3.08)
UDS	0.06	26.5 (H)	600 (Chandra)	4	1	8	117 (25)	5010	(−15.05, 4.90)
COSMOS	1.27	24 (K_s)	160 (Chandra)	3	2	5,10	1459 (880)	86765	(−14.68, 5.19)
ELAIS-S1	2.93	23.5 (K_s)	30 (XMM-Newton)	7	3	6,12	676 (261)	157791	(−13.90, 4.57)
W-CDF-S	4.23	23.5 (K_s)	30 (XMM-Newton)	7	3	6,12	872 (311)	210727	(−13.86, 4.97)
XMM-LSS	4.20	23.5 (K_s)	40 (XMM-Newton)	2	3	2	1765 (898)	254687	(−14.09, 5.36)
eFEDS	59.75	22 (Z)	2 (eROSITA)	1	2	3,7	2667 (1156)	615068	(−13.51, 2.59)

Wedding-cake surveys design

Up to 8000 AGNs in 1.3 million galaxies

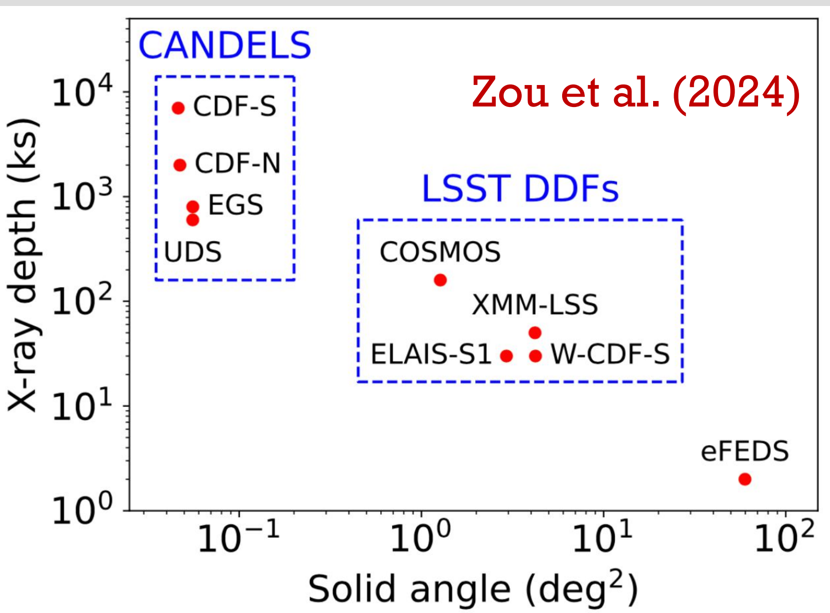

Long-term SMBH growth traced with the X-ray data, by averaging over samples.

Galaxy properties measured from the extensive multiwavelength data via, e.g., FIR-to-X-ray SED fitting.

Non-parametric partial-correlation analyses used to determine what correlations are fundamental.

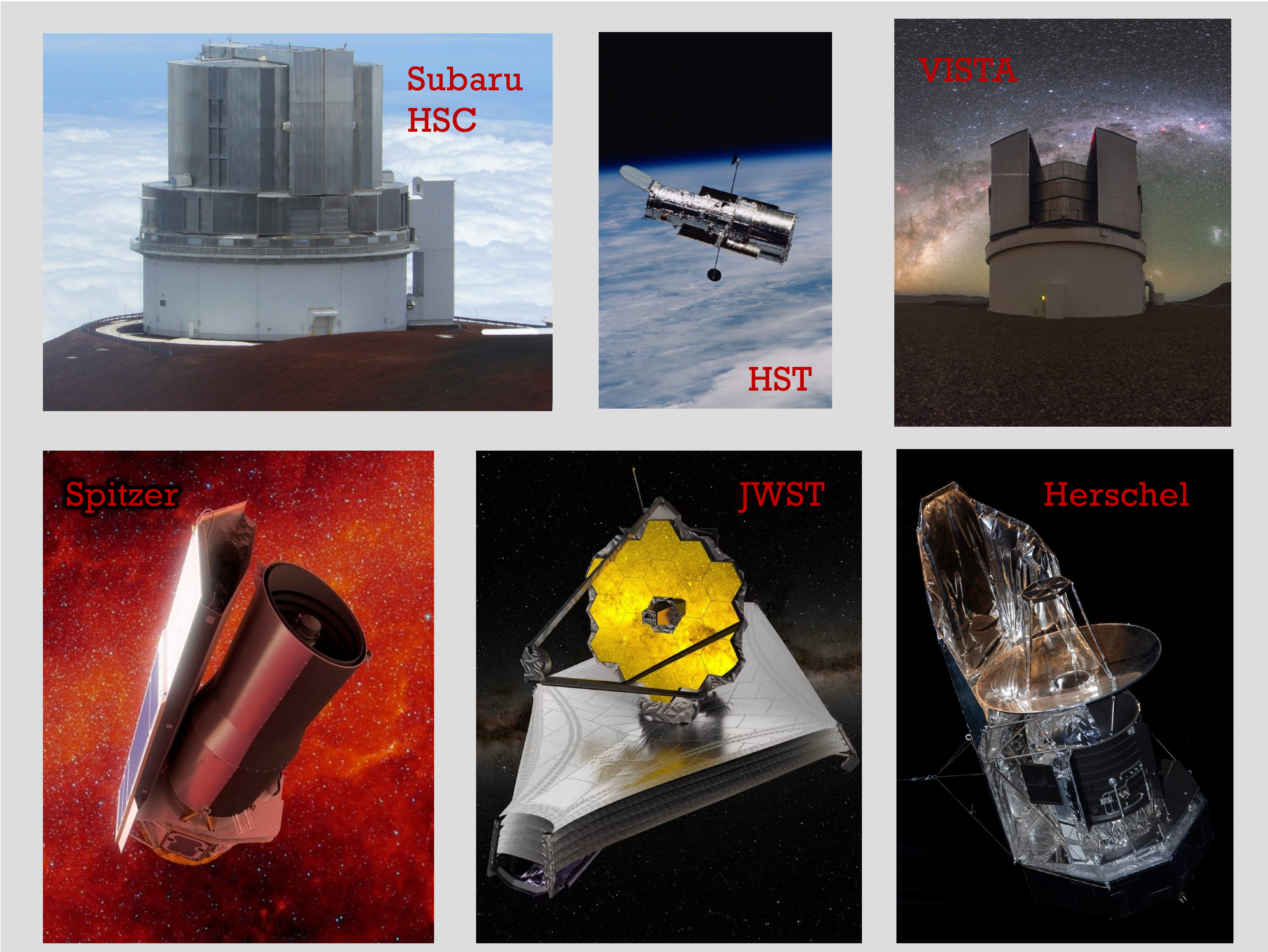
Subaru
HSC
HST
VISTA
Spitzer
JWST
Herschel

Surveys Used and Techniques

Table 1. Basic Information for the Fields Used in This Work

Field	Area (deg^2)	m_{lim} (AB mag)	X-ray Depth (ks)	X-ray ref.	Galaxy ref.	Photo-z ref.	AGN	Galaxies	(a, b)
(1)	(2)	(3)	(4)	(5)	(6)	(7)	(8)	(9)	(10)
GOODS-S	0.05	26.5 (H)	7000 (Chandra)	5	1	4,8	224 (111)	4144	(−15.87, 2.63)
GOODS-N	0.05	26.5 (H)	2000 (Chandra)	8	1	1,11	174 (167)	4603	(−15.49, 2.58)
EGS	0.06	26.5 (H)	800 (Chandra)	6	1	9	112 (10)	5889	(−15.13, 3.08)
UDS	0.06	26.5 (H)	600 (Chandra)	4	1	8	117 (25)	5010	(−15.05, 4.90)
COSMOS	1.27	24 (K_s)	160 (Chandra)	3	2	5,10	1459 (880)	86765	(−14.68, 5.19)
ELAIS-S1	2.93	23.5 (K_s)	30 (XMM-Newton)	7	3	6,12	676 (261)	157791	(−13.90, 4.57)
W-CDF-S	4.23	23.5 (K_s)	30 (XMM-Newton)	7	3	6,12	872 (311)	210727	(−13.86, 4.97)
XMM-LSS	4.20	23.5 (K_s)	40 (XMM-Newton)	2	3	2	1765 (898)	254687	(−14.09, 5.36)
eFEDS	59.75	22 (Z)	2 (eROSITA)	1	2	3,7	2667 (1156)	615068	(−13.51, 2.59)

Wedding-cake surveys design

Up to 8000 AGNs in 1.3 million galaxies

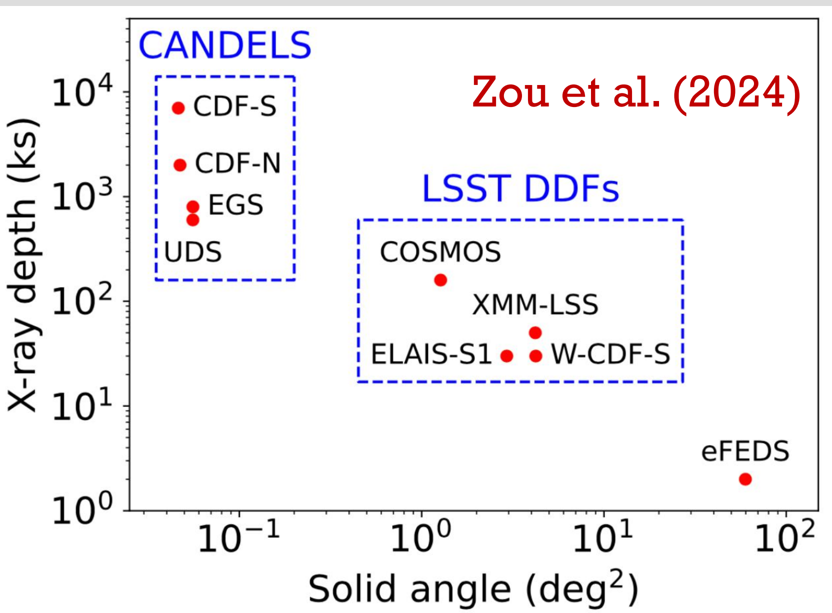

Long-term SMBH growth traced with the X-ray data, by averaging over samples.

Galaxy properties measured from the extensive multiwavelength data via, e.g., FIR-to-X-ray SED fitting.

Non-parametric partial-correlation analyses used to determine what correlations are fundamental.

Galactic Correlates

Stellar Mass

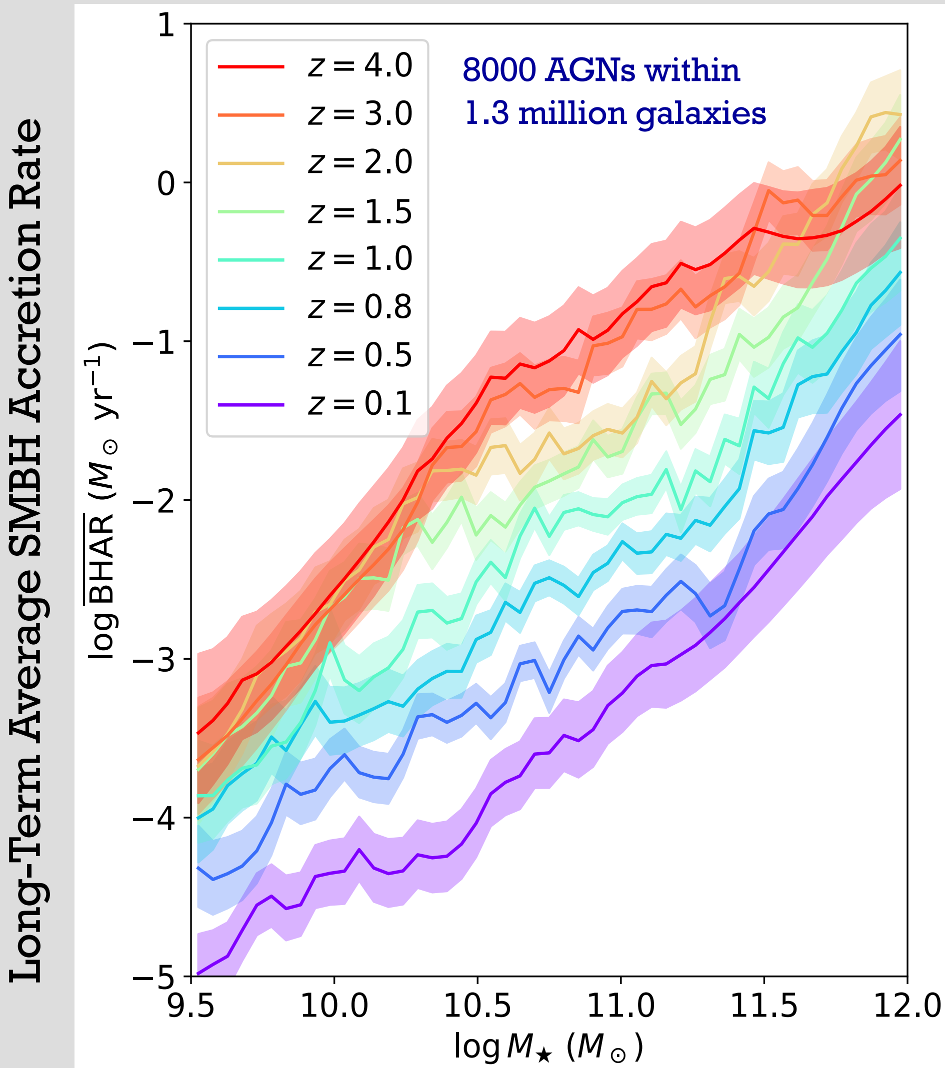

e.g. Zou et al. (2024); Yang et al. (2018)

For the general galaxy population at z = 0.1-4, long-term SMBH growth correlates most strongly with M_*

This dependence spans ~ 3 orders of magnitude in average black-hole accretion rate.

Also note the clear redshift dependence.

Stellar Mass

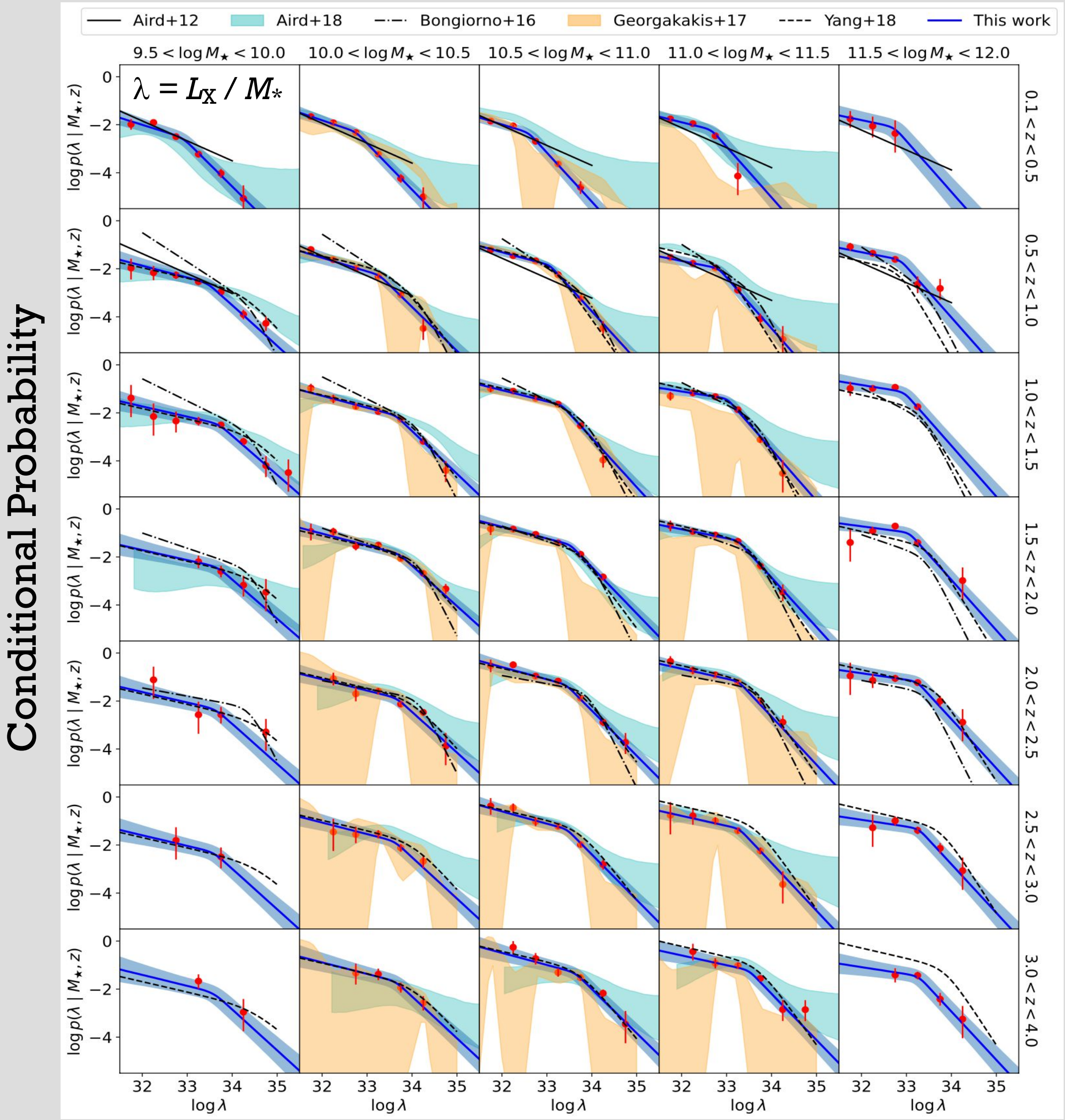

We also tightly constrain the underlying conditional probability distributions of λ over wide ranges of stellar mass and redshift.

Encodes much information about SMBH growth.

$$\overline{\mathrm{BHAR}}(M_\star, z) = \int_{\log \lambda_{\min}}^{+\infty} \frac{(1-\epsilon) k_{\mathrm{bol}}(M_\star \lambda) M_\star \lambda}{\epsilon c^2} p(\lambda \mid M_\star, z) d \log \lambda$$

Zou et al. (2024)

Bulge Star-Formation Rate

$M_\bullet$ tightly related to bulge M_* – but *not* tightly related to total M_* or disk M_*

$$\frac{d}{dt}$$

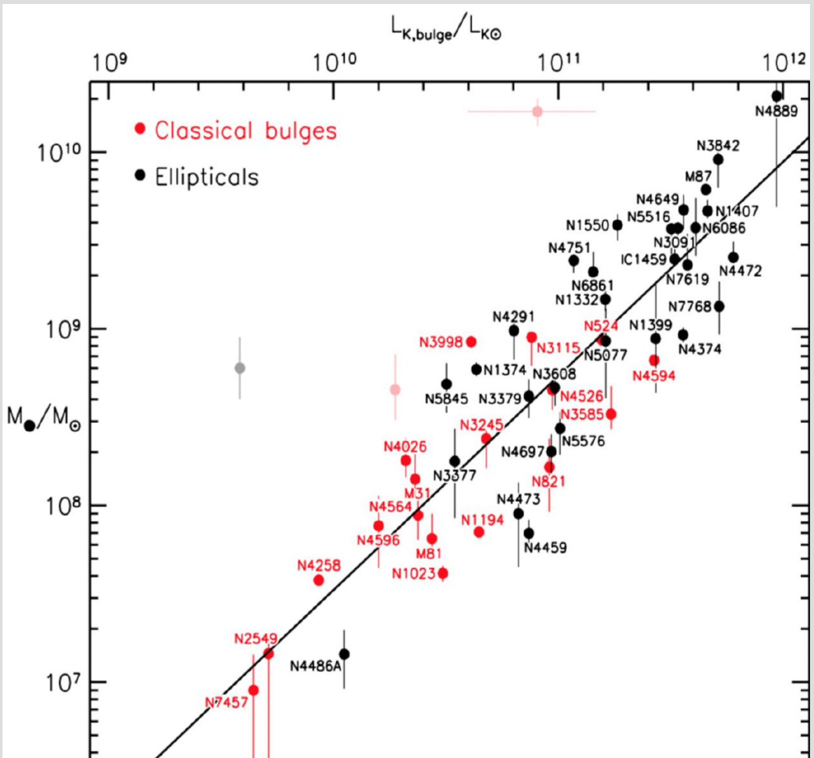

e.g., Kormendy & Ho (2013)

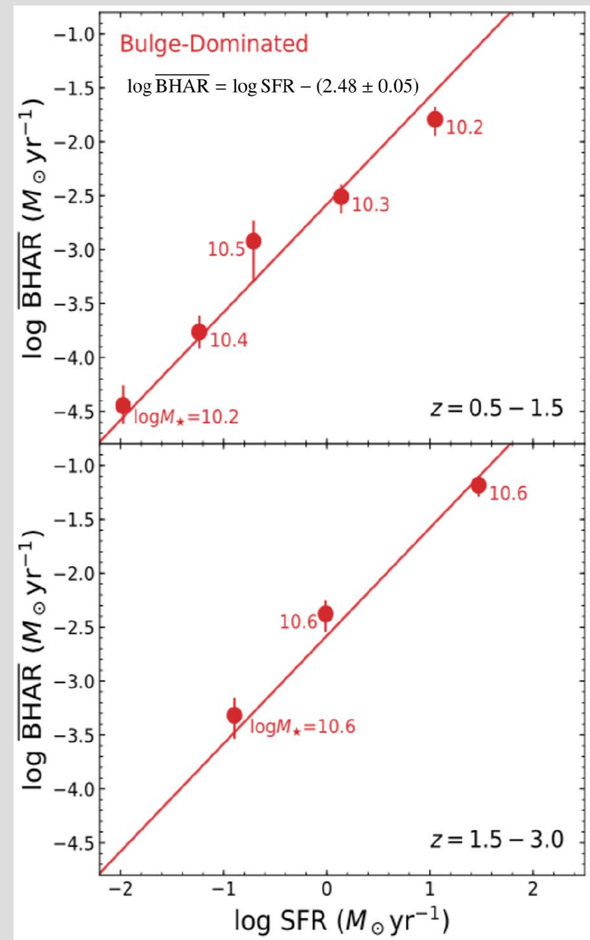

Yang et al. (2019)

Compactness

Compactness is a measure of the mass/size ratio of galaxies

$$\Sigma_1 = \frac{M_*(< 1\ \text{kpc})}{\pi\ (1\ \text{kpc})^2}$$

At least for gas-rich, star-forming galaxies, Σ_1 may also serve as a tracer of central-gas density on a kpc-scale.

Compactness Examples for log M_* ~ 10.3

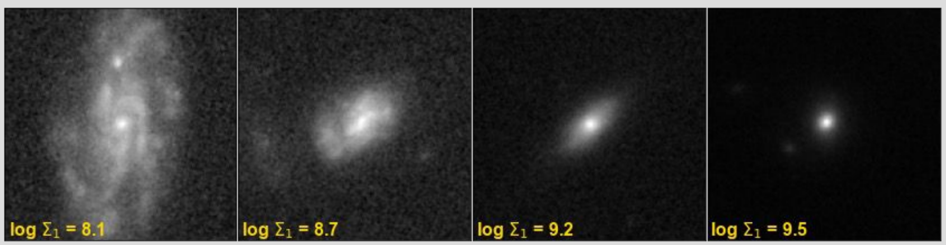

z = 0.3-0.5   COSMOS I-band

BHAR vs. Compactness for Star-Forming Galaxies

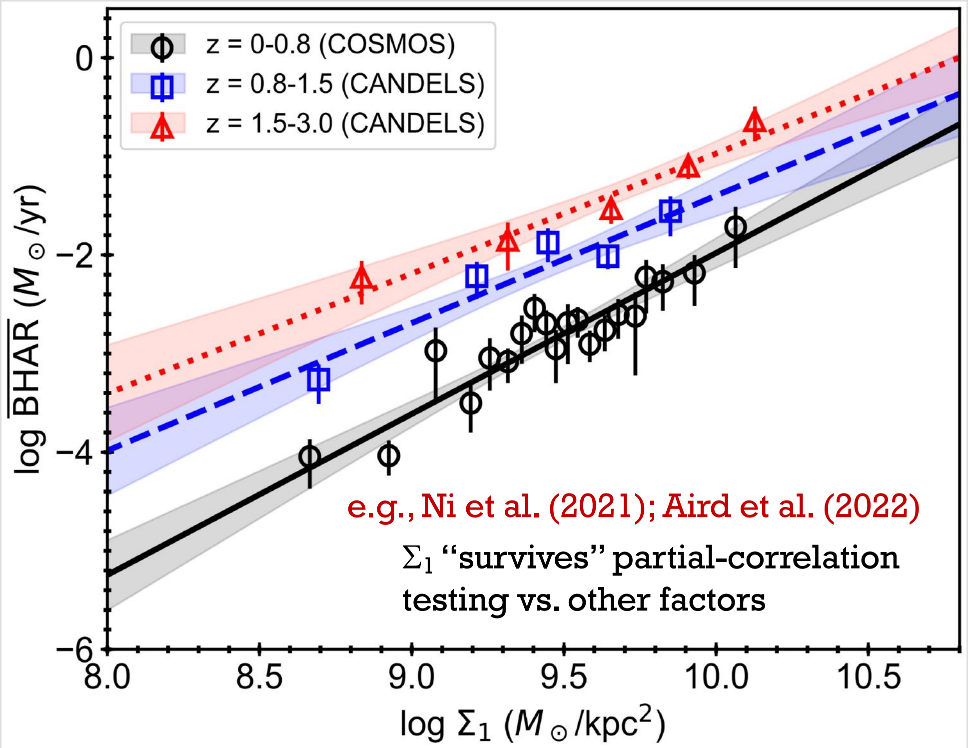

Not seen for quiescent galaxies, suggesting the role of gas density.

Redshift dependence can also be understood via gas evolution.

Their Application

The Astrophysical Journal, 976:6 (23pp), 2024 November 20 https://doi.org/10.3847/1538-4357/ad815d

The Cosmic Evolution of the Supermassive Black Hole Population: A Hybrid Observed Accretion and Simulated Mergers Approach

Fan Zou[1,2,3], W. N. Brandt[2,3,4], Elena Gallo[1], Bin Luo[5,6], Qingling Ni[7], Yongquan Xue[8,9], and Zhibo Yu[2,3]
[1] Department of Astronomy, University of Michigan, 1085 S University, Ann Arbor, MI 48109, USA; fanzou01@gmail.com
[2] Department of Astronomy and Astrophysics, 525 Davey Lab, The Pennsylvania State University, University Park, PA 16802, USA
[3] Institute for Gravitation and the Cosmos, The Pennsylvania State University, University Park, PA 16802, USA
[4] Department of Physics, 104 Davey Laboratory, The Pennsylvania State University, University Park, PA 16802, USA
[5] School of Astronomy and Space Science, Nanjing University, Nanjing, Jiangsu 210093, People's Republic of China
[6] Key Laboratory of Modern Astronomy and Astrophysics (Nanjing University), Ministry of Education, Nanjing 210093, People's Republic of China
[7] Max-Planck-Institut für extraterrestrische Physik (MPE), Gießenbachstraße 1, D-85748, Garching bei München, Germany
[8] CAS Key Laboratory for Research in Galaxies and Cosmology, Department of Astronomy, University of Science and Technology of China, Hefei 230026, People's Republic of China
[9] School of Astronomy and Space Sciences, University of Science and Technology of China, Hefei 230026, People's Republic of China
Received 2024 June 27; revised 2024 September 10; accepted 2024 September 23; published 2024 November 11

Abstract

Supermassive black holes (SMBHs) can grow through both accretion and mergers. It is still unclear how SMBHs evolve under these two channels from high redshifts to the SMBH population we observe in the local Universe. Observations can directly constrain the accretion channel but cannot effectively constrain mergers yet, while cosmological simulations provide galaxy merger information but can hardly return accretion properties consistent with observations. In this work, we combine the observed accretion channel and the simulated merger channel, taking advantage of observations and cosmological simulations, to depict a realistic evolution pattern of the SMBH population. With this methodology, we can derive the scaling relation between the black hole mass ($M_{\rm BH}$) and host-galaxy stellar mass ($M_\star$), and the local black hole mass function (BHMF). Our scaling relation is lower than those based on dynamically measured $M_{\rm BH}$, supporting the claim that dynamically measured SMBH samples may be biased. We show that the scaling relation has little redshift evolution. The BHMF steadily increases from $z=4$ to $z=1$ and remains largely unchanged from $z=1$ to $z=0$. The overall SMBH growth is generally dominated by the accretion channel, with possible exceptions at high mass ($M_{\rm BH} \gtrsim 10^8\,M_\odot$ or $M_\star \gtrsim 10^{11}\,M_\odot$) and low redshift ($z \lesssim 1$). We also predict that around 25% of the total SMBH mass budget in the local Universe may be locked within long-lived, wandering SMBHs, and the wandering mass fraction and wandering SMBH counts increase with $M_\star$.

Evolution of the SMBH Population: A Hybrid Approach

Observations constrain accretion channel well
(but not yet merger channel).

Simulations provide reasonable merger channel
(but unreliable accretion channel).

Observed accretion + Simulated mergers

BHAR(M_*, z) + IllustrisTNG

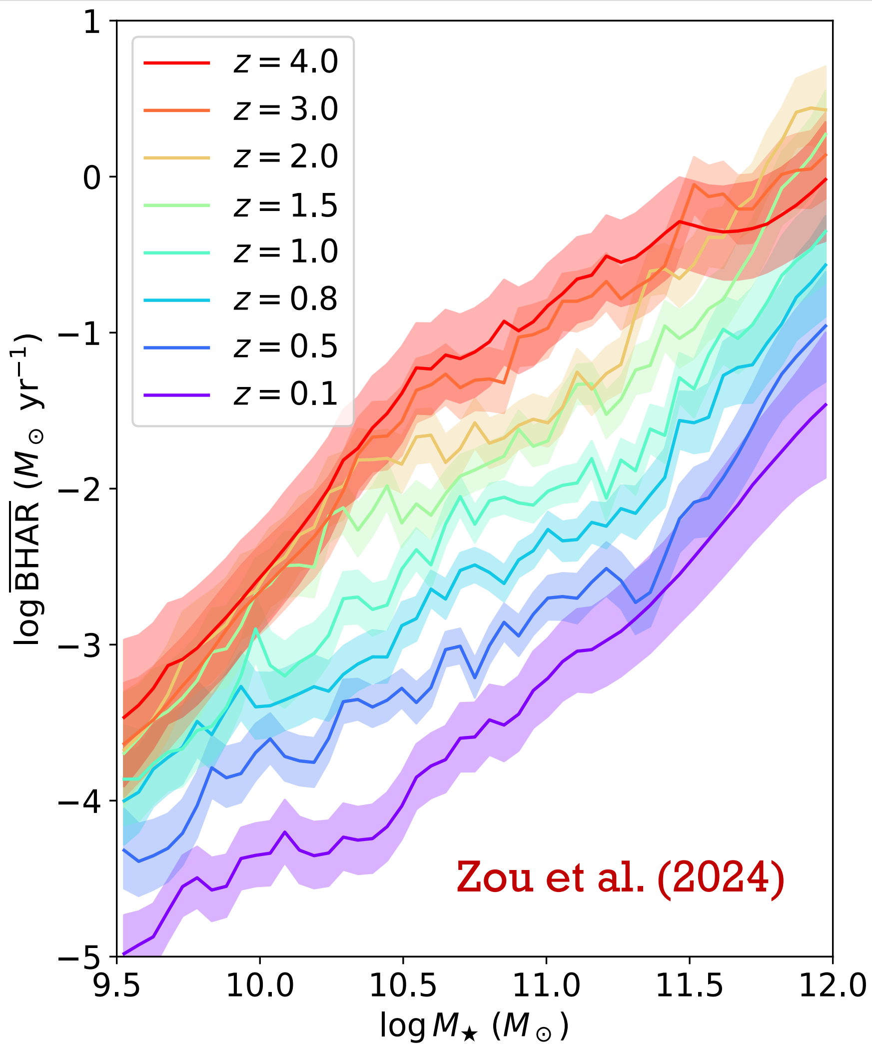

+

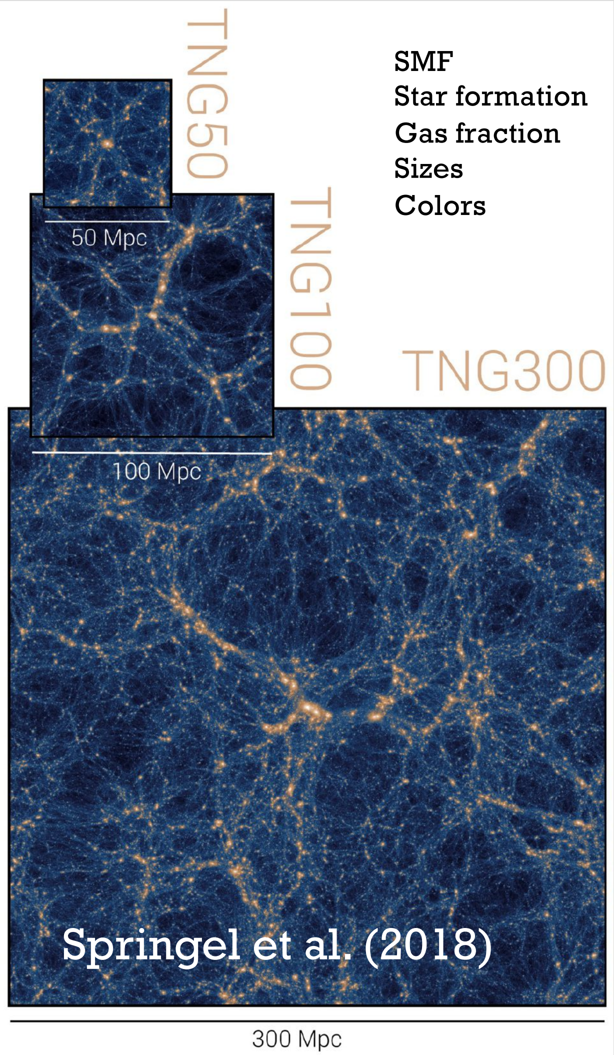

Track SMBH growth at z = 0-4 due to both observed accretion and IllustrisTNG mergers.

SMBH Mass Function

Mass Function Build-Up

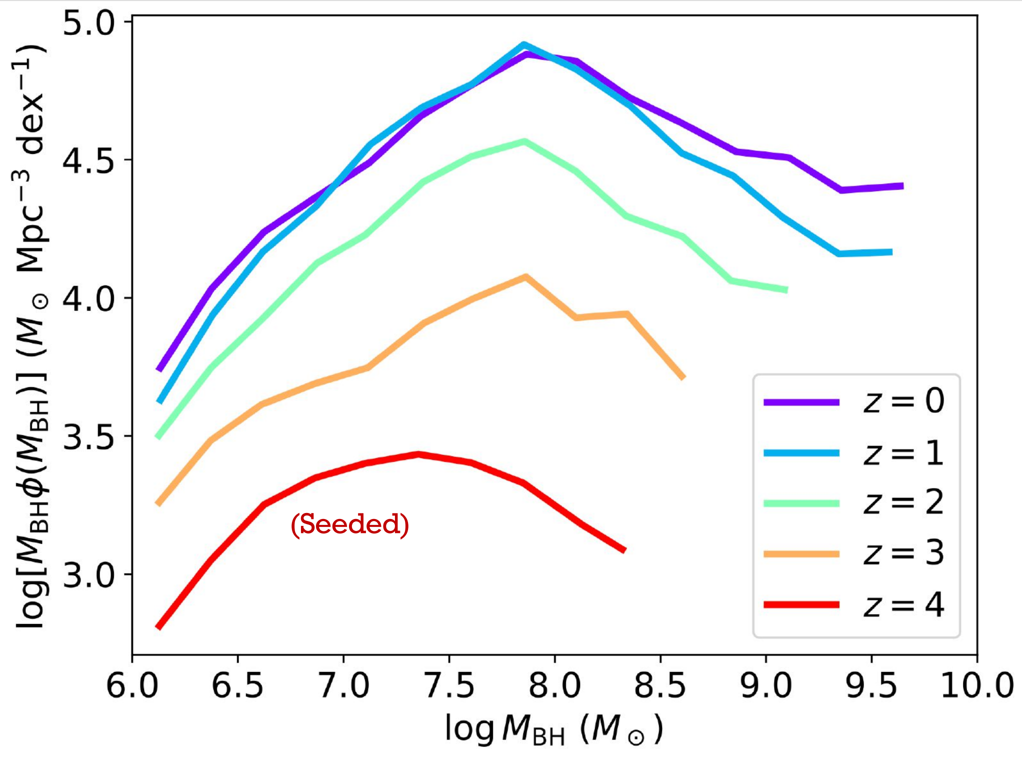

Where Is the Mass?

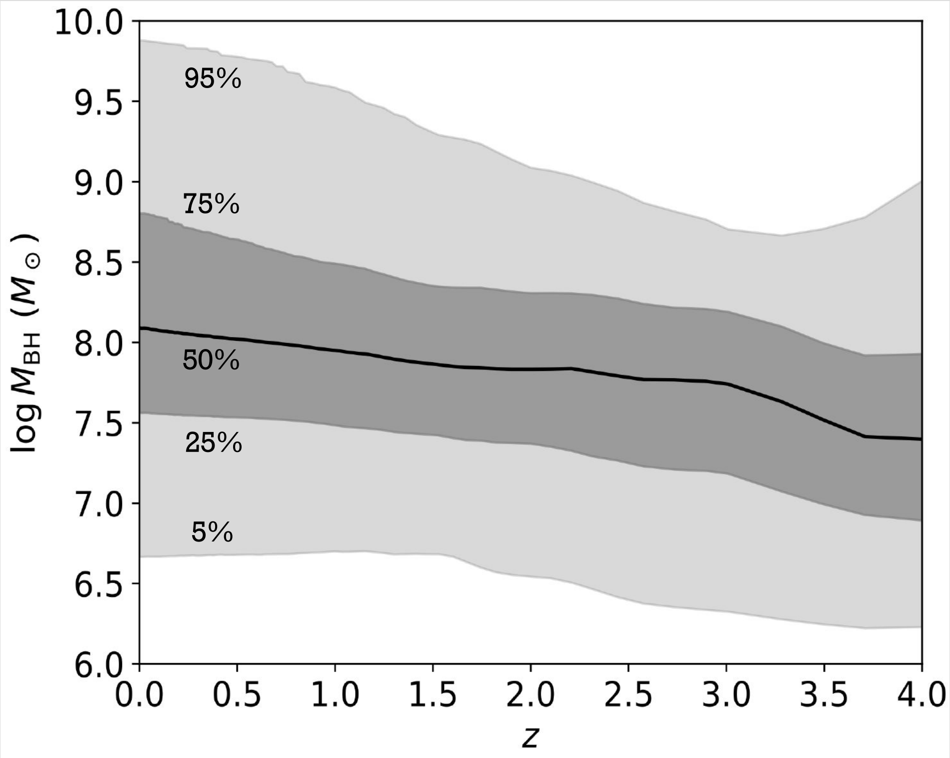

Zou et al. (2024)

300 M_{BH} from SDSS-RM

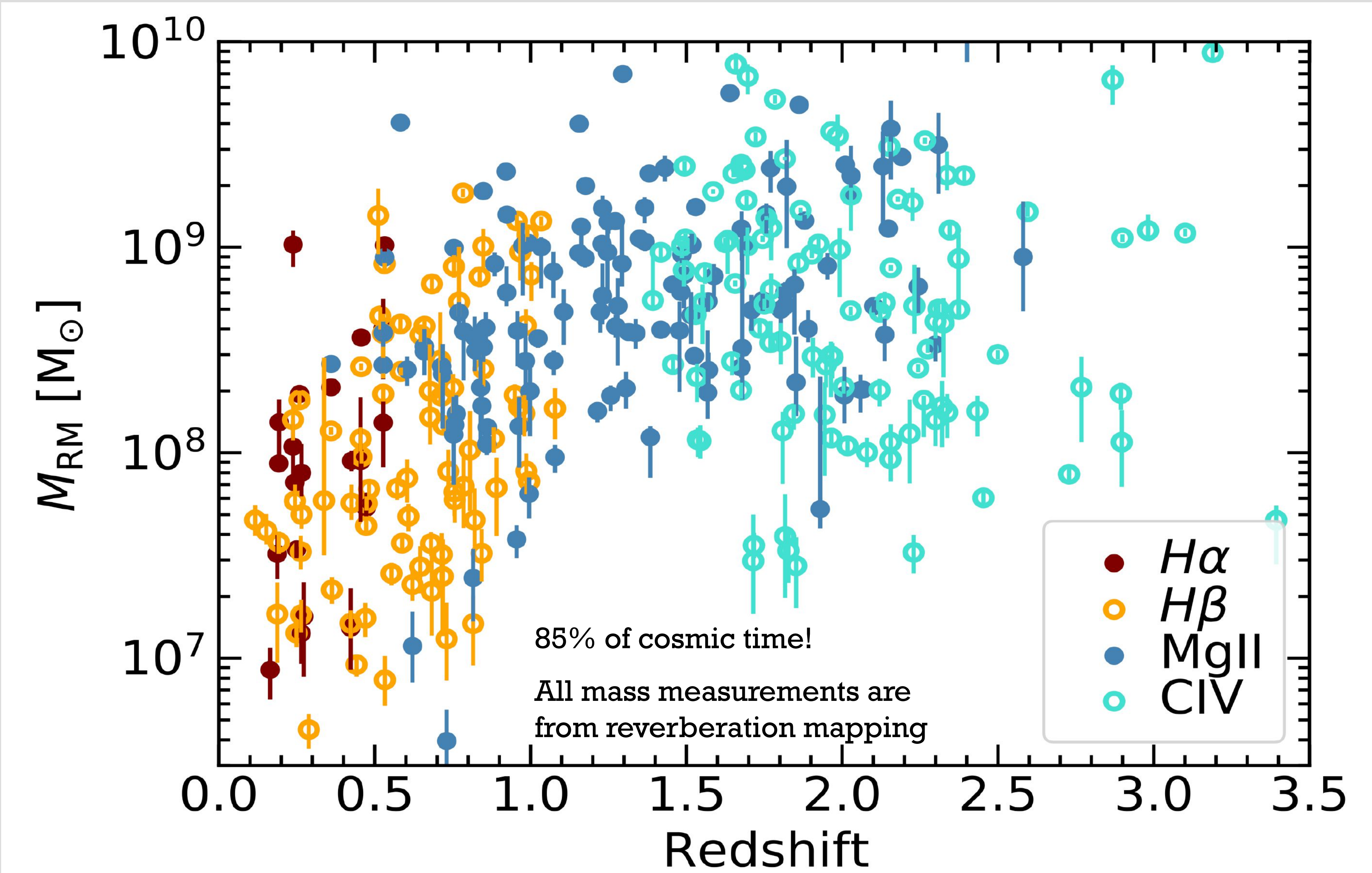

Shen et al. (2016, 2023); Grier et al. (2017, 2019); Homayouni et al. (2020)

Accretion vs. Mergers

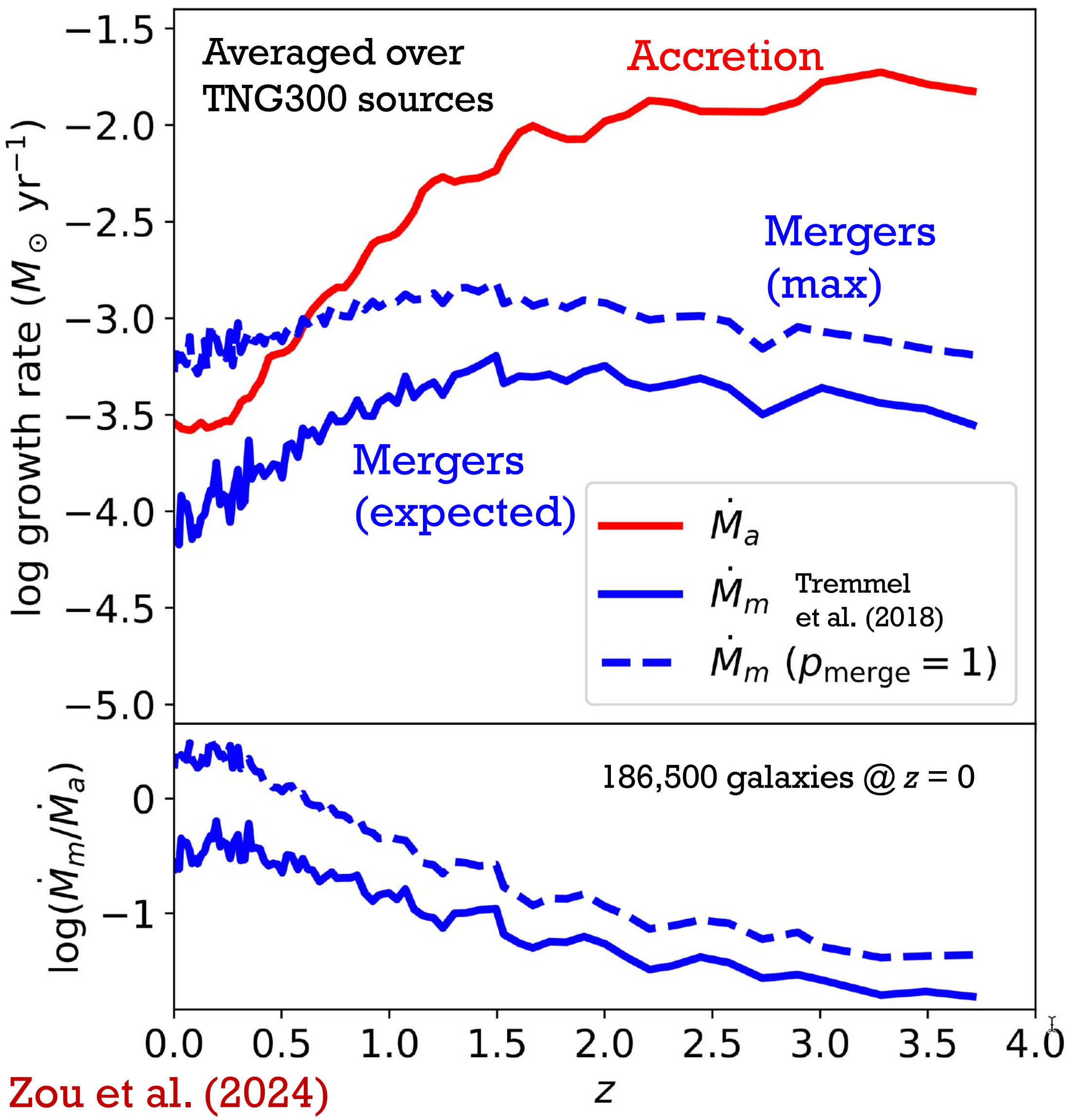

Zou et al. (2024)

Mergers become increasingly important toward low redshift.

But even at $z \sim 0$ they most likely contribute at ~ 30% level.

M_{BH}-M_* Relation

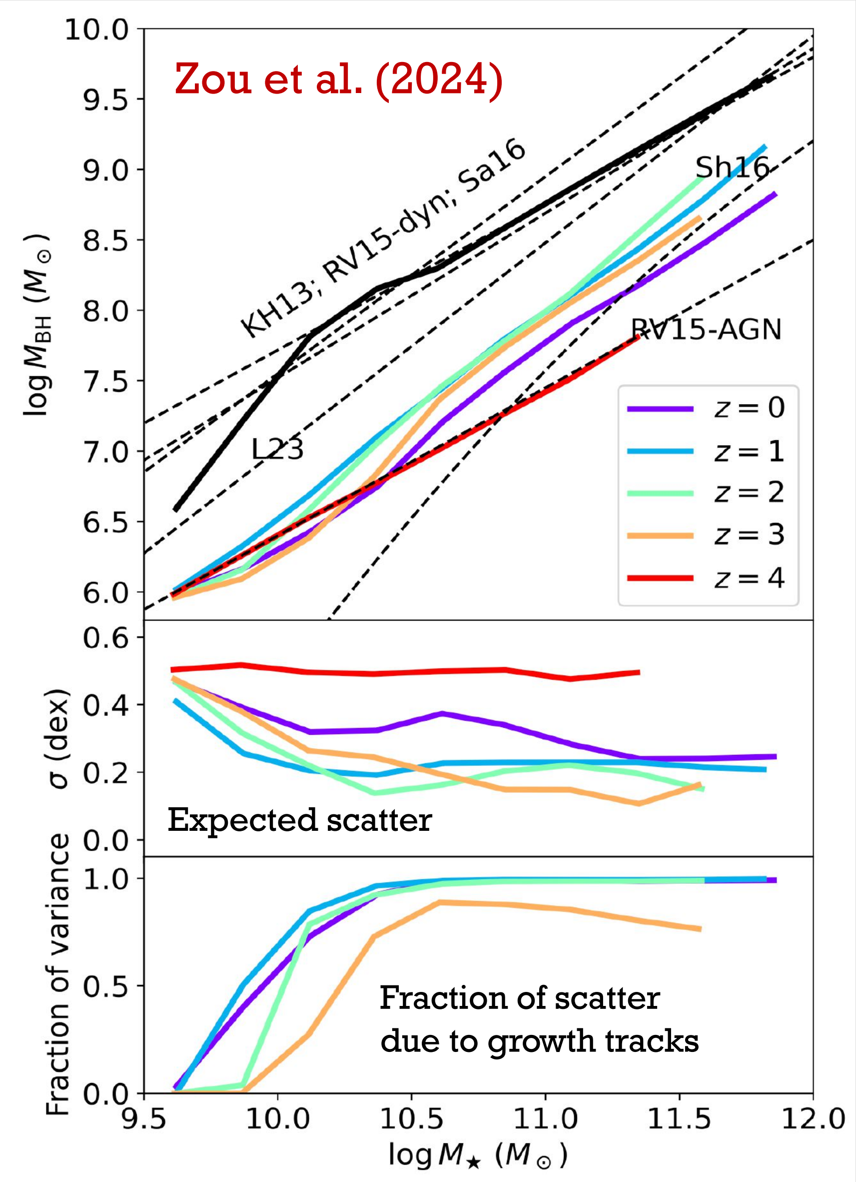

Recovered M_{BH}-M_* relation is lower than dynamically measured ones, agreeing better with those from broad-line AGNs.

Agrees better with the "de-biased" relation of Shankar et al. (2016, 2020).

The M_{BH}-M_* relation does not evolve much over z = 0-3, consistent with other constraints.

We also calculate the M_{BH} scatter, which can explain much of the observed scatter.

Our Galaxy's SMBH in Context

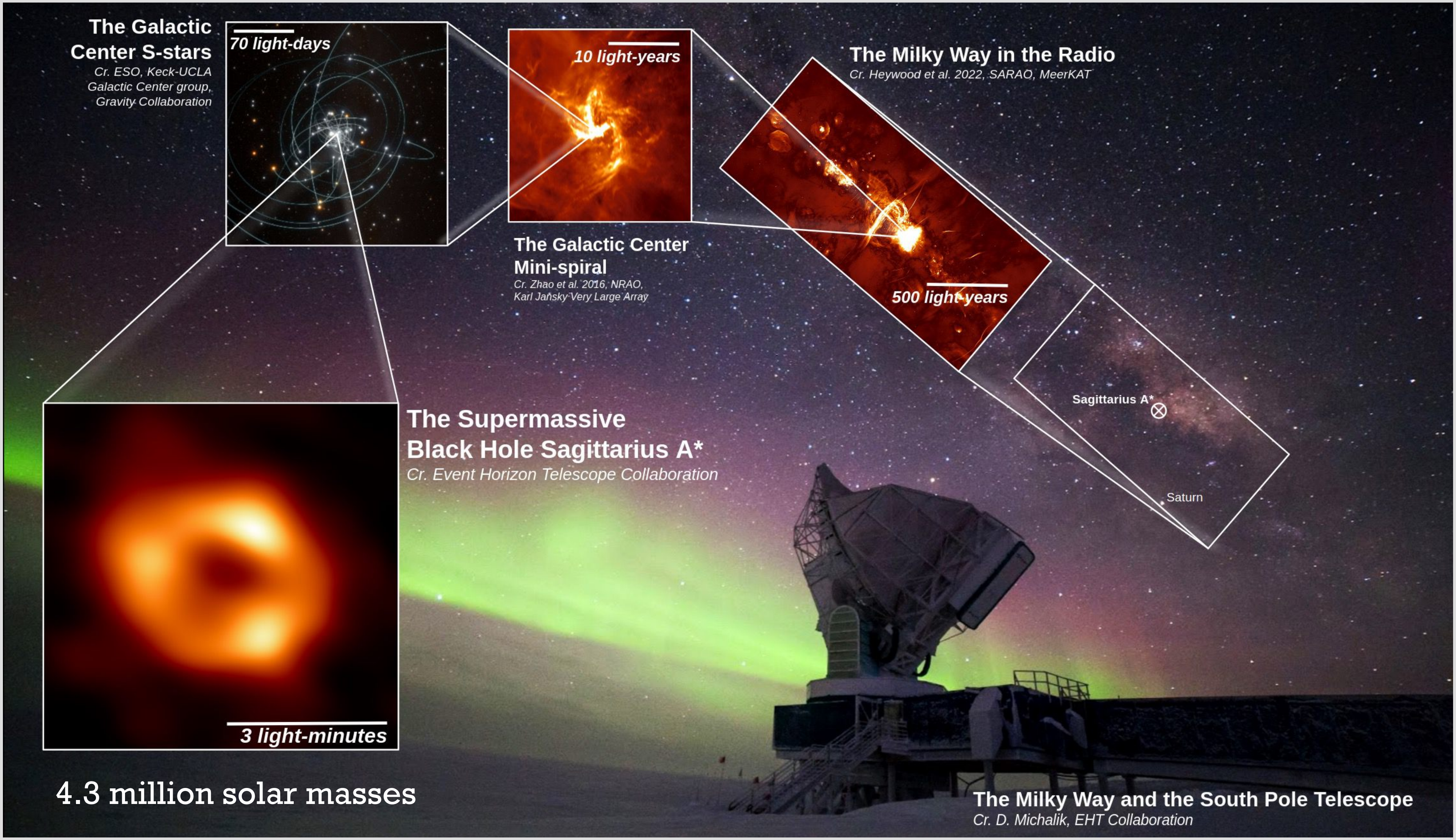

Galactic SMBH in Context

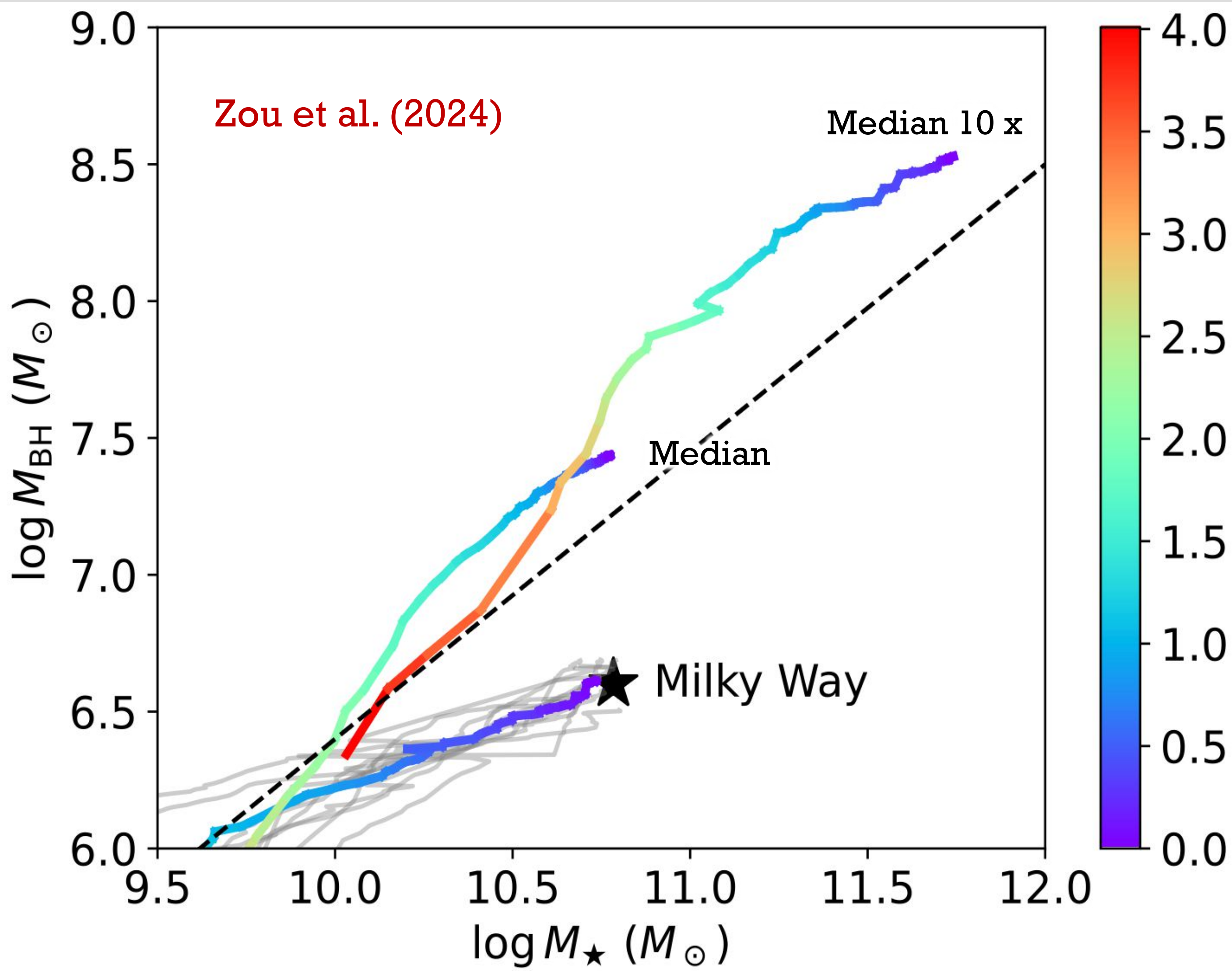

Galactic SMBH is ~ 7 times under-massive compared to median M_{BH} for other galaxies with similar M_*

Likely due to growth at lower redshift, when there is less BHAR at a given M_*

But not a strong outlier due to fairly large M_{BH} scatter (and other variance sources).

Future Prospects

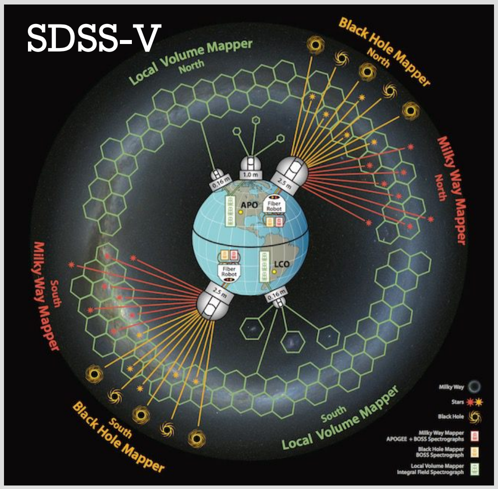

Prime Focus Spectrograph
SuMIRe

4MOST
WAVES
wide area vista extragalactic survey

LMT
ToITEC
ASU Cardiff INAOE Michigan NIST Northwestern UMass Wisconsin

The End

Please see the cited papers for many important details.

W-CDF-S XMM-Newton false-color image

Extra Slides

Cosmic Environment

0.1-1 Mpc Scales

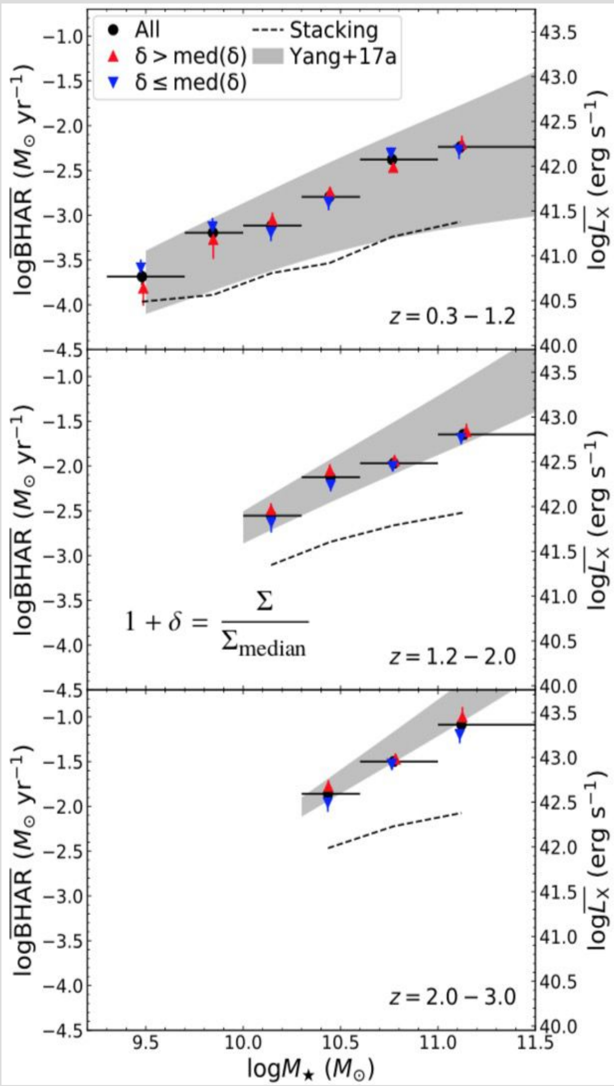

1-10 Mpc Scales

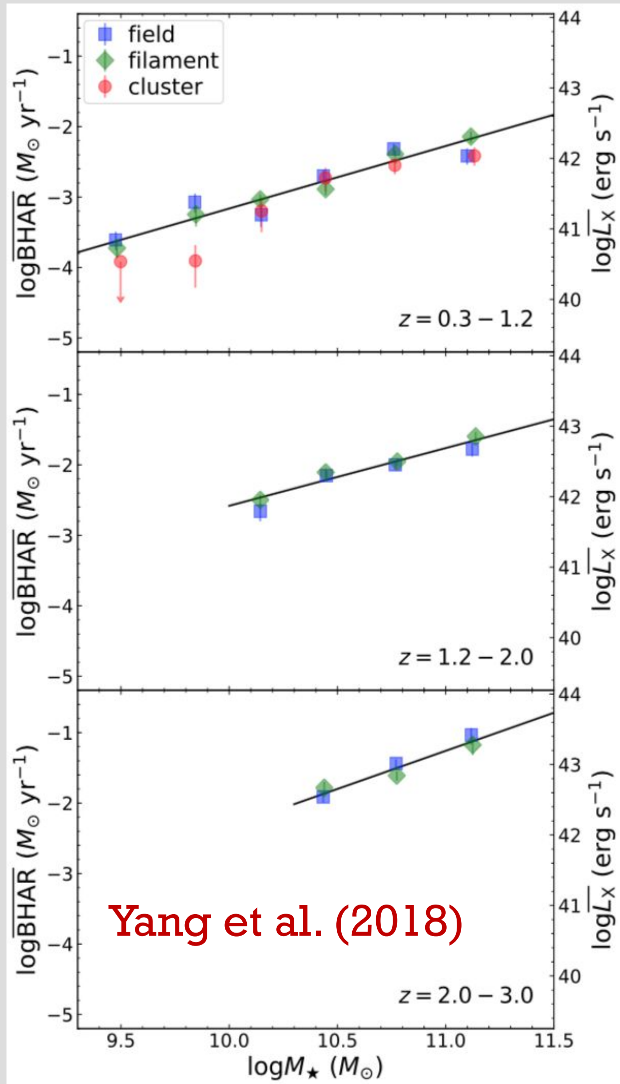

Using COSMOS UltraVISTA

Probe environments from field to $M_{\mathrm{Halo}} \sim 10^{14}\ M_\odot$ clusters

M_* is linked with environment

Partial-correlation testing shows M_* easily beats environment

Any environmental enhancement arises because massive galaxies tend to live in rich environments

Must push above $M_{\mathrm{Halo}} \sim 10^{14}\ M_\odot$ with LSST DDFs and MOONS – to connect to targeted protoclusters

IllustrisTNG Accretion Channel Issues

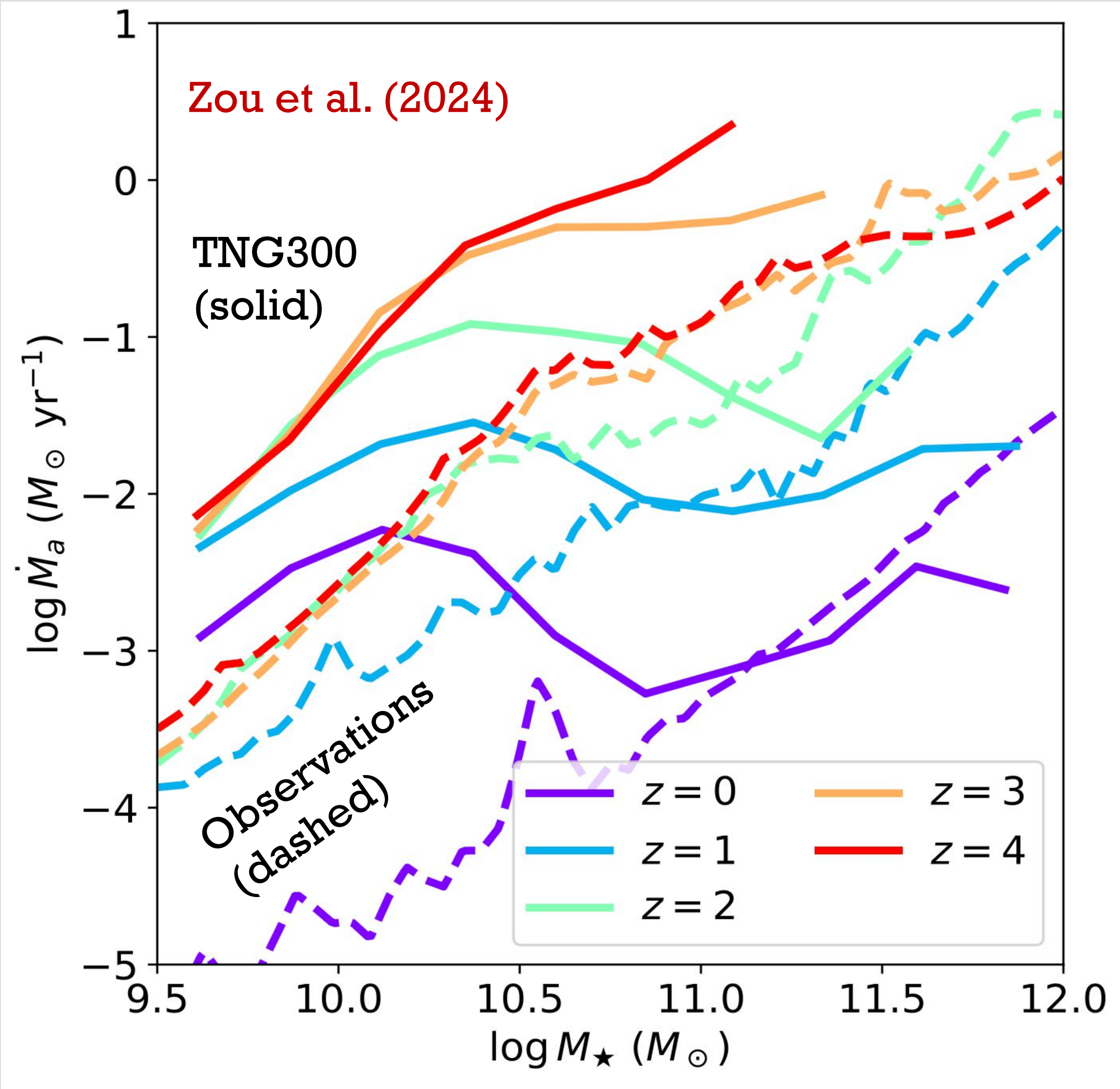

Sub-grid accretion physics in IllustrisTNG likely needs improvement – also see Habouzit et al. (2021,2022).

Eddington-limited Bondi-Hoyle accretion – with kinetic/thermal feedback included.

Compare Anglés-Alcázar colloquium.

BHAR(M_*, z) + IllustrisTNG

Observations

$$M_{\mathrm{BH},i}(z-\delta z) = M_{\mathrm{BH},i}(z) + \dot{M}_a(M_{\star,i}(z), z)\delta t + M_{\mathrm{BH},i}^{\mathrm{merger}}(z \rightarrow z - \delta z)$$

Simulations

- Start solving at $z = 4$, and sensitivity to initial conditions fades rapidly above ~ 10^{10} $M_\odot$.
- Initial seeding uses the M_{BH}-M_* relation of Reines & Volonteri (2015).
- Time step from TNG is ~ 0.15 Gyr.
- We track the *mean* SMBH accretion growth, averaging out accretion variations.
- Merger growth is derived for the most-massive SMBH along the merger tree.
- p_{merge} for mergers from Tremmel et al. (2018) - also set upper limits for $p_{\mathrm{merge}} = 1$.

Merger Probability

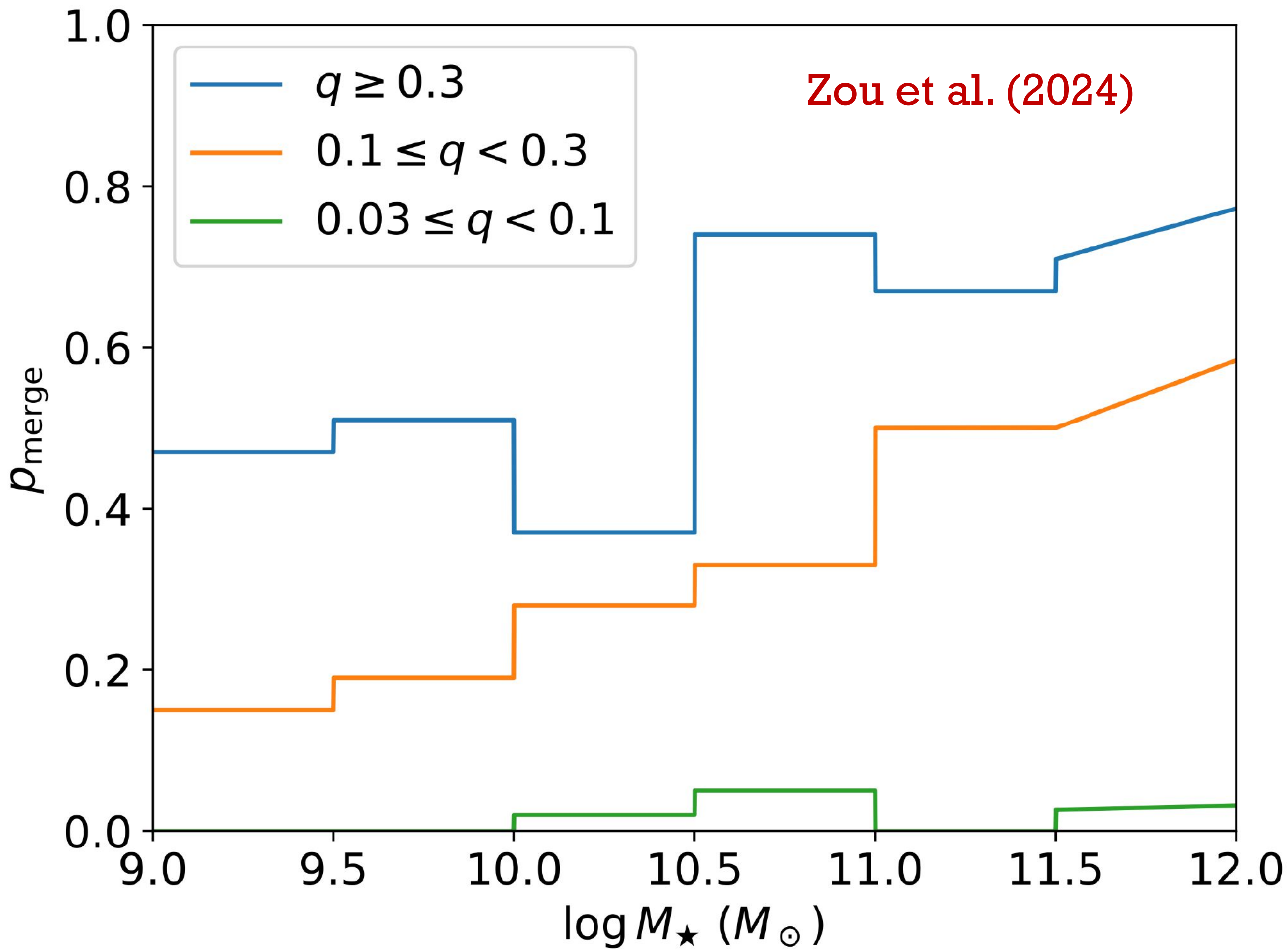

Figure 1. Our adopted $p_{\rm merge}$ based on M. Tremmel et al. (2018b) as a function of $M_\star$ at different q bins. Term $p_{\rm merge}$ is set to 0 for $q < 0.03$ and is extrapolated only in the massive end ($M_\star > 10^{11.5}\ M_\odot$).

SMBH Masses vs. Redshift

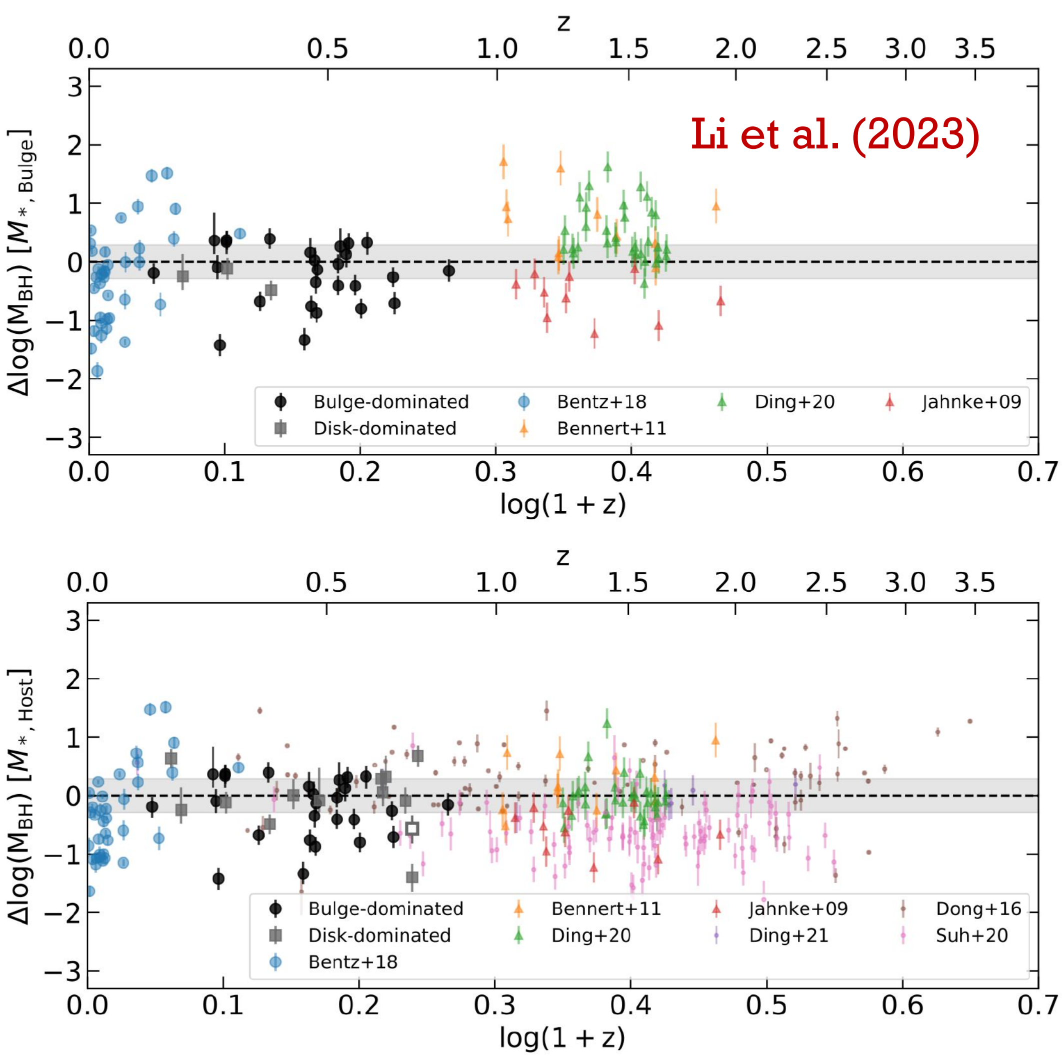

Figure 10. Evolution of $\Delta\log(\mathrm{M_{BH}})$ with redshift, with baselines adopted from the best-fit relations of $M_{\rm BH} - M_{\rm Bulge}$ and $M_{\rm BH} - L_{\rm Bulge}$ from the Kormendy & Ho (2013) sample. Our work is the only sample with RM-based BH masses beyond $z > 0.3$. Vertical error bars are from uncertainties in BH mass only.